Scientific Research Publishing

Open Journal of Radiology, 2020, 10, 9-15
https://www.scirp.org/journal/ojrad
ISSN Online: 2164-3032
ISSN Print: 2164-3024

Can Gd-EOB-DTPA Affect Proton Density Fat Fraction Using 6-Point DIXON Methods? A Multicenter, Multivendor Phantom Study

Tatsuya Hayashi[1*], Kei Fukuzawa[2], Hidekazu Yamazaki[3], Takashi Konno[3], Jun'ichi Kotoku[1], Satoshi Saitoh[4]

[1]Graduate School of Medical Technology, Teikyo University, Tokyo, Japan
[2]Department of Radiological Technology, Toranomon Hospital, Tokyo, Japan
[3]Department of Radiological Technology, Southern TOHOKU General Hospital, Fukushima, Japan
[4]Department of Hepatology, Toranomon Hospital, Tokyo, Japan
Email: *t-hayashi@med.teikyo-u.ac.jp

How to cite this paper: Hayashi, T., Fukuzawa, K., Yamazaki, H., Konno, T., Kotoku, J. and Saitoh, S. (2020) Can Gd-EOB-DTPA Affect Proton Density Fat Fraction Using 6-Point DIXON Methods? A Multicenter, Multivendor Phantom Study. *Open Journal of Radiology*, **10**, 9-15.
https://doi.org/10.4236/ojrad.2020.101002

Received: January 14, 2020
Accepted: February 10, 2020
Published: February 13, 2020

Abstract

Purpose: To evaluate the influence of gadolinium ethoxybenzyl diethylenetriamine pentaacetic acid (Gd-EOB-DTPA) on proton density fat fraction (PDFF) using multiple vendors' DIXON methods in a multicenter, multivendor phantom study. **Materials and Methods:** Pairs of phantoms with varying fat volume percentages (0, 5, 10, 15, 20, 30, 40, and 50) and Gd-EOB-DTPA concentrations (0 and 0.4 mM) were constructed. The phantom without Gd-EOB-DTPA in each pair was defined as the precontrast phantom, and the corresponding phantom with Gd-EOB-DTPA in each pair was defined as the postcontrast phantom. The phantoms were scanned via three vendors' DIXON techniques to determine PDFFs. Agreement between PDFFs determined in precontrast and postcontrast phantoms was evaluated via Bland–Altman analysis. **Results:** Mean differences (precontrast PDFF - postcontrast PDFF) and limits of agreement were Philips 5.1% (−0.8% to 11.0%), Siemens 6.1% (−0.9% to 13.1%), and GE 1.3% (−1.2% to 3.9%). **Conclusions:** PDFFs measured using the three vendors' DIXON techniques were smaller in the postcontrast phantoms than in the corresponding precontrast phantoms regardless of different scanning parameters, because T1 bias was improved by Gd-EOB-DTPA.

Keywords

Dixon, Fat, Liver, MRI, Phantom, Quantification

1. Introduction

Nonalcoholic fatty liver disease is a common cause of chronic liver disease worldwide [1]. It includes nonalcoholic fatty liver and nonalcoholic steatohepatitis (NASH). Nonalcoholic fatty liver entails a small risk of associated cirrhosis, whereas NASH entails a much greater risk of cirrhosis, which can progress to hepatocellular carcinoma [2] [3]. Although liver management and monitoring treatment responses in patients with NASH require a liver biopsy, it is a potentially invasive procedure that is occasionally associated with complications and mortality [4].

Magnetic resonance imaging (MRI) is a noninvasive, quantitative, and repeatable method for assessing liver fat. Water and fat proton densities are used to quantify liver fat, via a parameter defined as the proton density fat fraction (PDFF). One MRI method called DIXON utilizes chemical shift between water and fat protons. However, several factors can confound the accurate determination of PDFF, including T1 bias (which refers to the longer T1 of water compared to fat), T2* decay, the multipeak spectral complexity of fat, and others [5]. To minimize the influence of these factors, a low flip angle to minimize T1 bias, multi-echo techniques to correct T2* decay, and a multipeak fat model are used in the latest DIXON methods [5] [6] [7] [8]. Many vendors now offer multi-echo DIXON techniques for PDFF, but the scanning parameters used in these techniques are not the same. In a previous study, PDFFs calculated by different vendors' 3T MRI machines were consistent with each other even when the same scanning parameters were not used [9]. Although generally, PDFF is acquired from non-contrast liver, recent reports suggest that PDFFs determined via post-gadolinium ethoxybenzyl diethylenetriamine pentaacetic acid (Gd-EOB-DTPA) contrast imaging are more accurate because of improvement of T1 bias and a high signal-to-noise ratio [10] [11]. Notably, however, the influence of Gd-EOB-DTPA on PDFF has not been evaluated in a multivendor study in various clinical settings.

The purpose of the current study was to evaluate the influence of Gd-EOB-DTPA on PDFF using multiple vendors' prescribed DIXON methods in a multicenter, multivendor phantom study.

2. Materials and Methods

2.1. Phantoms

The phantoms used in the current study were the same phantoms used in previously reported studies [9] [11] [12]. Duplicate vegetable oil (mixture of soybean and rapeseed oil) and water phantoms were constructed with fat volume percentages of 0, 5, 10, 15, 20, 30, 40, and 50. One of each pair contained no Gd-EOB-DTPA, and the other contained 0.4 mM Gd-EOB-DTPA. Phantoms without Gd-EOB-DTPA were defined as precontrast phantoms and those with Gd-EOB-DTPA were defined as postcontrast phantoms. A small amount of soy lecithin was used to prepare homogenous emulsions of fat and water. Further

details of these phantoms are described in previous reports [9] [11] [12] [13].

2.2. MRI

The 3T MRI machines and DIXON sequences used were the Ingenia (Philips Healthcare, Best, The Netherlands), mDIXON Quant; the Skyra (Siemens Healthcare, Erlangen, Germany), q-DIXON, and the Discovery MR750w (GE Healthcare, Waukesha, Wis, USA), IDEAL IQ. Scanning parameters are shown in Table 1. All data were acquired when those of a previous research we conducted were obtained; thus, the data derived from precontrast phantoms is consistent with that in a previous report [9]. All DIXON sequences used 6-echo for T2* decay correction, a low flip angle to minimize T1 bias, and a multipeak fat model. The optimum T2* and the signal intensities of water and fat at a TE of 0 ms were calculated from the signal intensities of multiecho images. The PDFF map was generated automatically from the signal intensities of water and fat. Regions of interest (ROIs) were placed in the center of the phantom, and PDFFs were measured. The average of three scans was used in the analysis.

2.3. Statistical Analysis

Bland-Altman analysis was used to evaluate agreement between precontrast and postcontrast PDFF in each machine. In the Bland-Altman analysis, 95% limits of agreement (LOA) were defined as the mean difference ± 1.96 × the standard deviation. All statistical analyses were performed using BellCurve for Excel version 2.11 (Social Survey Research Information Co., Ltd., Tokyo, Japan).

3. Results

The precontrast and postcontrast PDFFs are summarized in Table 2. Representative PDFF maps are shown in Figure 1. For all DIXON methods, the postcontrast PDFFs were smaller than the corresponding precontrast PDFFs. Bland-Altman plots representing comparisons between precontrast and postcontrast PDFFs are shown in Figure 2. The mean differences (precontrast PDFF - postcontrast PDFF) were Philips 5.1% (LOA −0.8% to 11.0%), Siemens 6.1% (LOA −0.9% to 13.1%), and GE 1.3% (LOA −1.2% to 3.9%).

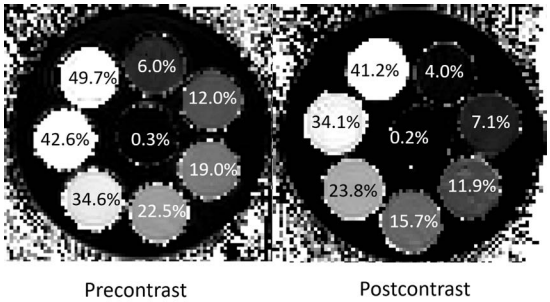

Figure 1. Representative proton density fat fraction maps in precontrast and postcontrast phantoms. Each pixel represents the proton density fat fraction. Proton density fat fractions are smaller in the postcontrast phantom than in the precontrast phantom.

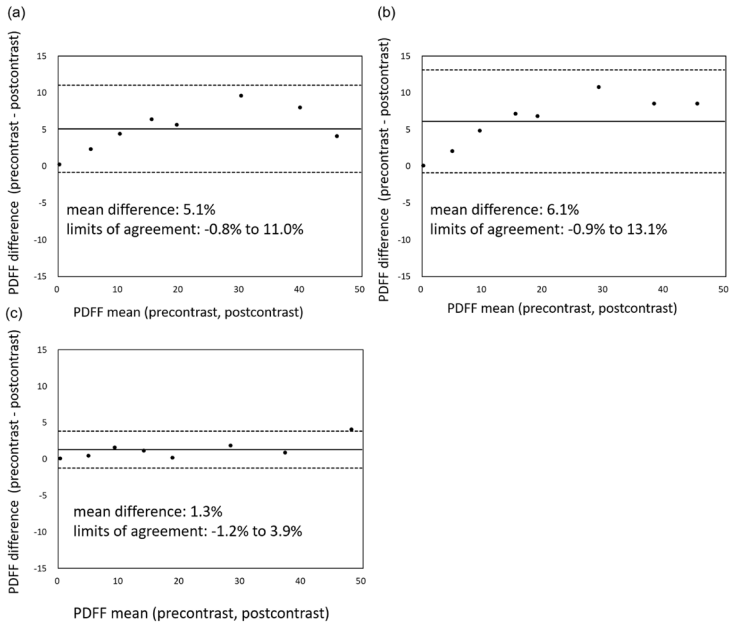

Figure 2. Bland–Altman plots of proton density fat fractions comparing precontrast and postcontrast phantoms. (a) Philips; (b) Siemens; and (c) GE. Solid lines represent mean difference, and dotted lines represent 1.96 × the standard deviation (limit of agreement).

Table 1. Magnetic resonance imaging parameters used in different DIXON methods.

Vendor	TR (ms)	TE (ms)	ETL	Flip Angle (degree)	Slice Thickness (mm)	FOV (cm^2)	Matrix
Philips	6.2	0.95, 1.75, 2.55, 3.35, 4.15, 4.95	6	3	5	280 × 220	112 × 88
Siemens	9.0	1.05, 2.46, 3.69, 4.92, 6.15, 7.38	6	4	5	300 × 300	128 × 128
GE	19.3	0.90, 2.46, 4.02, 5.58, 7.14, 8.70	6	3	5	280 × 220	112 × 88

TR, repetition time; TE, echo time; ETL, echo train length; FOV, field of view.

Table 2. Proton density fat fraction in precontrast and postcontrast phantoms using the DIXON methods prescribed by three different vendors.

Fat volume	Philips		Siemens		GE	
	Precontrast	Postcontrast	Precontrast	Postcontrast	Precontrast	Postcontrast
0%	0.3%	0.1%	0.3%	0.2%	0.4%	0.3%
5%	6.6%	4.2%	6.0%	4.0%	5.2%	4.7%
10%	12.4%	8.0%	12.0%	7.1%	10.1%	8.5%
15%	18.7%	12.3%	19.0%	11.9%	14.7%	13.5%
20%	22.5%	16.8%	22.5%	15.7%	18.9%	18.7%
30%	35.1%	25.5%	34.6%	23.8%	29.3%	27.4%
40%	44.0%	35.9%	42.6%	34.1%	37.8%	36.9%
50%	48.1%	44.0%	49.7%	41.2%	50.3%	46.2%

4. Discussion

In this multivendor, multicenter study all PDFFs measured using the different vendors' DIXON techniques were smaller in the postcontrast phantoms than in the corresponding precontrast phantoms. The results are consistent with those of a previous single vendor study [12]. It is important for medical doctors and technicians to know that Gd-EOB-DTPA has similar effects in various DIXON techniques with different clinical MRI parameters.

Previous authors have reported that the respective T1 values of water and fat are 933 ms and 361 ms in precontrast liver [14]. The difference in T1 between water and fat is called "T1 bias". Accurate PDFF measurements require the elimination of this bias; thus, low flip angle sequences are recommended. Notably, however, a low flip angle is associated with noise in PDFF measurements [6]. In contrast, in Gd-EOB-DTPA postcontrast liver, the respective T1 values of water and fat are 358 ms and 359 ms [14]. The administration of Gd-EOB-DTPA decreases water's T1 but not fat's T1, which improves T1 bias [10] [11]. Longitudinal magnetization relaxation of water occurs more rapidly in postcontrast conditions than in precontrast conditions because of a shorter T1, which leads to a comparatively reduced postcontrast PDFF. Furthermore, Gd-EOB-DTPA improves the signal-to-noise ratio. These findings support the validity of the present study and suggest that postcontrast PDFF is theoretically more accurate. The postcontrast PDFFs were smaller in the postcontrast phantoms than in the corresponding fat volumes. Although, we were unable to measure the T1 of the water and the fat separately, the degree of T1 change of the water in the phantom may have been different to that in the liver. If the T1 of the water is less than that of the fat in the postcontrast phantom, the PDFF can be underestimated, as it was in this study. This subject needs a further investigation.

The current study had some limitations. MRI parameters among vendors are not unified, and this can influence evaluations conducted in actual clinical settings. Acquisition parameters are dependent on institutions; thus, PDFF ranges will differ in each institution. For example, under the current study's settings the precontrast-postcontrast change in PDFF determined using the GE machine was smaller than those determined using the other vendors' machines. Repetition time (TR) is one of the parameters that determine the degree of the T1 weighted image. Under the current study's settings, repetition time using the GE machine was two to three times longer than those of the other machines, and this may have influenced the results. The degree of change in PDFF will vary from institution to institution.

5. Conclusion

The PDFFs measured using the vendors' DIXON techniques were smaller in the postcontrast phantoms than in the corresponding precontrast phantoms regardless of different scanning parameters, because T1 bias was improved by Gd-EOB-DTPA.

Acknowledgements

The authors would like to thank Takahide Okamoto, Hiroshi Onodera, Shuji Toyotaka, Rie Tojo, Shimpei Yano, and Mika Kokubun for assistance with the experiments.

Funding

This research received no specific grant from any funding agency in the public, commercial, or not-for-profit sectors.

Conflicts of Interest

None.

References

[1] Caussy, C., Reeder, S.B., Sirlin, C.B. and Loomba, R. (2018) Noninvasive, Quantitative Assessment of Liver Fat by MRI-PDFF as an Endpoint in NASH Trials. *Hepatology*, **68**, 763-772. https://doi.org/10.1002/hep.29797

[2] Ratziu, V., Bonyhay, L., Di Martino, V., *et al.* (2002) Survival, Liver Failure, and Hepatocellular Carcinoma in Obesity-Related Cryptogenic Cirrhosis. *Hepatology*, **35**, 1485-1493. https://doi.org/10.1053/jhep.2002.33324

[3] Adams, L.A., Lymp, J.F., St Sauver, J., *et al.* (2005) The Natural History of Nonalcoholic Fatty Liver Disease: A Population-Based Cohort Study. *Gastroenterology*, **29**, 113-121. https://doi.org/10.1053/j.gastro.2005.04.014

[4] West, J. and Card, T.R. (2010) Reduced Mortality Rates Following Elective Percutaneous Liver Biopsies. *Gastroenterology*, **139**, 1230-1237. https://doi.org/10.1053/j.gastro.2010.06.015

[5] Reeder, S.B. and Sirlin, C.B. (2010) Quantification of Liver Fat with Magnetic Resonance Imaging. *Magnetic Resonance Imaging Clinics of North America*, **18**, 337-357. https://doi.org/10.1016/j.mric.2010.08.013

[6] Liu, C.Y., McKenzie, C.A., Yu, H., Brittain, J.H. and Reeder, S.B. (2007) Fat Quantification with IDEAL Gradient Echo Imaging: Correction of Bias from T(1) and Noise. *Magnetic Resonance in Medicine*, **58**, 354-364. https://doi.org/10.1002/mrm.21301

[7] Meisamy, S., Hines, C.D., Hamilton, G., *et al.* (2011) Quantification of Hepatic Steatosis with T1-Independent, T2-Corrected MR Imaging with Spectral Modeling of Fat: Blinded Comparison with MR Spectroscopy. *Radiology*, **258**, 767-775. https://doi.org/10.1148/radiol.10100708

[8] Kühn, J.P., Hernando, D. and Muñoz del Rio, A. (2012) Effect of Multipeak Spectral Modeling of Fat for Liver Iron and Fat Quantification: Correlation of Biopsy with MR Imaging Results. *Radiology*, **265**, 133-142. https://doi.org/10.1148/radiol.12112520

[9] Hayashi, T., Fukuzawa, K., Yamazaki, H., *et al.* (2018) Multicenter, Multivendor Phantom Study to Validate Proton Density Fat Fraction and T2* Values Calculated Using Vendor-Provided 6-Point DIXON Methods. *Clinical Imaging*, **51**, 38-42. https://doi.org/10.1016/j.clinimag.2018.01.011

[10] Park, C.C., Hamilton, G., Desai, A., *et al.* (2017) Effect of Intravenous Gadoxetate Disodium and Flip Angle on Hepatic Proton Density Fat Fraction Estimation with Six-Echo, Gradient-Recalled-Echo, Magnitudebased MR Imaging at 3T. *Abdominal*

Radiology (NY), **42**, 1189-1198. https://doi.org/10.1007/s00261-016-0992-4

[11] Hayashi, T., Fukuzawa, K., Kondo, H., *et al.* (2018) Influence of Gd-EOB-DTPA on T1 Dependence of the Proton Density Fat Fraction Using Magnetic Resonance Spectroscopy. *Radiological Physics and Technology*, **11**, 338-344. https://doi.org/10.1007/s12194-018-0466-1

[12] Hayashi, T., Fukuzawa, K., Kondo, H., *et al.* (2017) Influence of Gd-EOB-DTPA on Proton Density Fat Fraction Using the Six-Echo Dixon Method in 3 Tesla Magnetic Resonance Imaging. *Radiological Physics and Technology*, **10**, 483-488. https://doi.org/10.1007/s12194-017-0420-7

[13] Fukuzawa, K., Hayashi, T., Takahashi, J., *et al.* (2017) Evaluation of Six Point Modified Dixon and Magnetic Resonance Spectroscopy for Fat Quantification: A Fat-Water-Iron Phantom Study. *Radiological Physics and Technology*, **10**, 349-358. https://doi.org/10.1007/s12194-017-0410-9

[14] Hamilton, G., Middleton, M.S., Cunha, G.M. and Sirlin, C.B. (2013) Effect of Gadolinium-Based Con Trast Agent on the Relaxation Properties of Water and Fat in Human Liver as Measured *in Vivo* by 1H MRS. *Proceedings International Society for Magnetic Resonance in Medicine*, **21**, 1516.